Lattice thermal conductivity of self-assembled PbTe-Sb_2Te_3 composites with nanometer lamellae

Teruyuki Ikeda[1], Eric S. Toberer[1], Vilupanur A. Ravi[2], Sossina M. Haile[1], G. Jeffrey Snyder[1]
[1]California Institute of Technology
1200 E. California Blvd., Pasadena, CA 91106, USA
[2]California State Polytechnic University
3801 W. Temple Avenue, Pomona, CA 91768, USA

Abstract

In the system of PbTe and Sb_2Te_3, a metastable compound $Pb_2Sb_6Te_{11}$ appears by solidification processing. It has been reported that heat treatments decomposes this compound into two immiscible thermoelectric materials forming nanosized lamellar structure. The fraction transformed and the inter-lamellar spacing was systematically investigated. In this work, the thermal conductivities and the electrical resistivities have been measured as functions of annealing time through the transformation and the coarsening processes to clarify the effect of the fraction transformed and the inter-lamellar spacing. The thermal conductivity of $Pb_2Sb_6Te_{11}$ is lower than that after the decomposition. The lattice part of the thermal conductivity of PbTe/Sb_2Te_3 lamellar samples decreases with deccreasing inter-lamellar spacing. This is considered to be due to the coarsening of the microstructure.

Introduction

In order for thermoelectric devices to be more commonly used in large industrial fields for effective use of heat or electrical energy, it is essential to discover materials with a high thermoelectric figure of merit, zT, defined as $S^2\sigma T/\kappa$, where S is the Seebeck coefficient, σ the electrical conductivity and κ the thermal conductivity. One way to improve a figure of merit zT is to introduce nano-sized structure into thermoelectric materials [1-3]. This is achieved presumably by enhanced phonon scattering [4], which decreases thermal conductivity κ. Here, we examine a system of two immiscible thermoelectric materials: PbTe-Sb_2Te_3. In this system, it has been shown that the metastable compound $Pb_2Sb_6Te_{11}$ appears at a composition close to that of the eutectic [5, 6] and decomposes into two thermoelectric compounds, PbTe and Sb_2Te_3, forming nano-sized lamellar structures [7, 8]. In the present work, eutectic PbTe-Sb_2Te_3 alloys were synthesized by quenching in a copper mold and then annealed at several temperatures to control the fraction transformed and inter-lamellar spacing. The electrical resistivity and the thermal conductivity of as-quenched and annealed samples have been investigated as functions of the spacing.

Experimental procedure

Samples with overall composition matching the $Pb_2Sb_6Te_{11}$ compound ($Pb_{10.5}Sb_{31.6}Te_{57.9}$) were prepared by injection molding. Stoichiometric quantities of Pb, Sb, and Te granules were loaded into 12mm fused silica ampoules and then sealed under a vacuum of approximately 4×10^{-3} Pa to prevent oxidation at high temperatures. Samples were then melted in vertical furnace for 5 min and were subsequently water quenched. They were then cut into small pieces with a diamond saw. The small pieces, 15-20 g in total, were put into a fused silica tube with 12 mm outer diameter and with a hole of approximately 1 mm diameter and were melted by induction heating under vacuum of approximately 4×10^{-3} Pa. When the sample melted, the sample dropped through the hole into a copper mold of $20 \times 30 \times$ mm^3. For property measurements, samples with size of typically 10×10 mm^2 were cut out with a diamond saw and then the surfaces were ground to remove the surface layers until the final thickness was around 1.5 mm.

Electrical resistivity and thermal conductivity measurements were carried out before and after annealing the samples. For annealing, samples were sealed under vacuum in fused silica tubes. The annealing temperature was 673 K (78 h, 150 h) or 773 K (1 h, 24 h, 126 h).

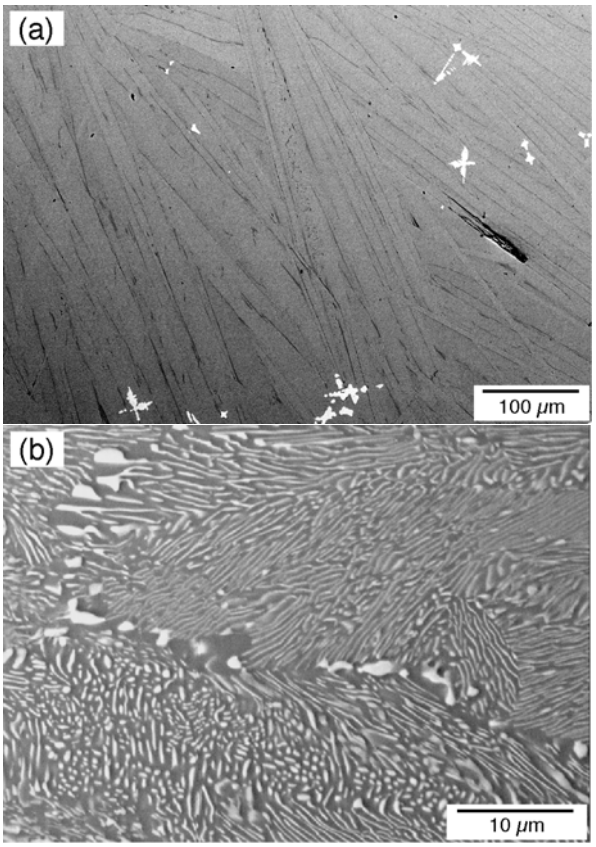

Figure 1: Microstructure of $Pb_{10.5}Sb_{31.6}Te_{57.9}$: (a) as quenched and (b) annealed at 673 K for 150 h.

978-1-4244-2263-0/08/$25.00 ©2008 IEEE.

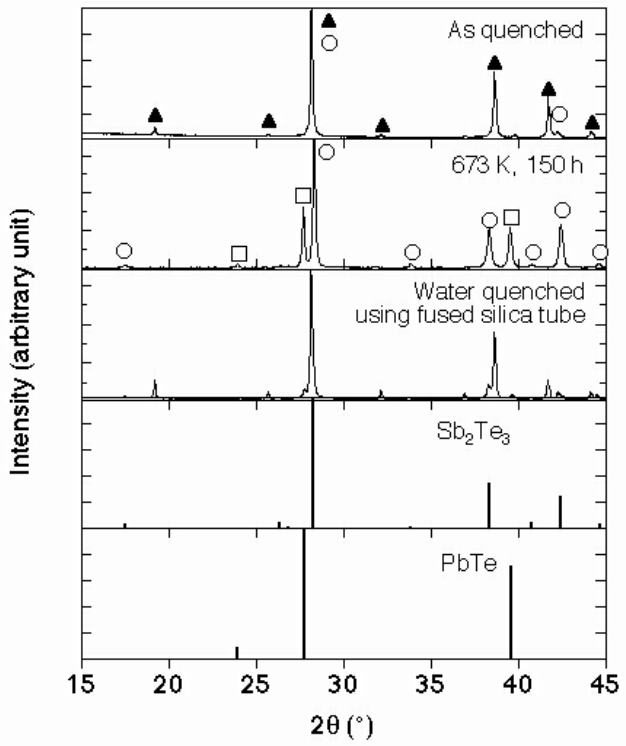

Figure 2: XRD profiles obtained from $Pb_{10.5}Sb_{31.6}Te_{57.9}$ as quenched and annealed at 673 K for 150 h. Open squares (□), open circles (○) and solid triangles (▲) show the peaks from PbTe, Sb_2Te_3 and $Pb_2Sb_6Te_{11}$ phases, respectively.

The electrical resistivity (ρ) was measured up to 523 K, below which microstructure is not considered to practically change during measurements because of low atomic diffusivity [8], using the van der Pauw method with a current of 10 mA as functions of temperature. The Hall coefficient (R_H) was measured in the same apparatus with a forward and reverse magnetic field value of ~9500 G. The carrier density (n) was calculated from the Hall coefficient assuming a scattering factor of 1.0 in a single-carrier scheme, with $n = 1/R_H e$, where n is the densities of charge carriers (holes) and e the charge of the electron.

The thermal diffusivities were measured up to 523 K using the same samples as the electrical resistivity measurements by flash diffusivity technique (LFA457, NETSZCH). The thermal conductivity (κ) was calculated from the thermal diffusivity which was experimentally measured and the heat capacity which was estimated using Dulong-Petit law.

The microstructures were observed using a field emission-scanning electron microscope (Carl Zeiss LEO 1550 VP) equipped with a backscattered electron (BSE) detector for its high compositional contrast capabilities. The accelerating voltage was 20 kV. The microstructures were digitally analyzed using an image analysis program (Macscope, Mitani Corp.) to determine the inter-lamellar spacing (ILS) and the fraction transformed (Y). X-ray diffraction (XRD) experiments (Phillips X-Pert Pro diffractometer, Cu K-α radiation, $15^\circ \leq 2\theta \leq 45^\circ$) were performed directly on the as-prepared ingots to identify phases.

Results and discussion

Microstructure

Figure 1 (a) and (b) show the microstructure of the samples which are as-quenched and after annealing at 673 K for 150 h, respectively. The sample in as-quenched state is almost entirely composed of the gray matrix phase, $Pb_2Sb_6Te_{11}$. The thin dark acicular phase is Sb_2Te_3 and the bright dendrites are PbTe. The phases composing of as-quenched and annealed samples were also checked by XRD experiments as shown in Fig. 2. These features were consistent with the solidification microstructure of this system by water-quenching using fused silica tubes [6]. The inter-lamellar spacing in the solidification structure was 13 μm in the vicinity of the sample surface and 16 μm in the middle, which were also consistent with that for water quenching using fused silica tube in the previous work. After annealing at 673 K for 78 h or at 773 K 126 h, $Pb_2Sb_6Te_{11}$ is almost completely decomposed to Sb_2Te_3 and PbTe as reported in the previous work [7]. The backscattered electron images were digitally analyzed to determine the fraction transformed (Y) and the inter-lamellar spacing (ILS). The results of the image analysis is summarized in Table 1. In the sample annealed at 673 K for 78 or 150 h and the one annealed at 773 K for 126 h, the transformation to $PbTe/Sb_2Te_3$ lamellar structure is almost complete. It is also found that ILS is increased by annealing.

Table 1. Fraction transformed (Y) and inter-lamellar spacing (ILS) of the samples annealed at 673 or 773 K.

Sample ID	Annealing condition		Y (%)	ILS (nm)	
	T / K	t / h		Average	Standard deviation
A	673	78	99.7	536	155
		150	100	575	153
B	773	1	88.7	544	168
		126	100	1591	487

Electrical resistivity

Figure 3 shows the electrical resistivity and the carrier concentration measured as functions of temperature. The resistivity is found to decrease by the decomposition of $Pb_2Sb_6Te_{11}$ to $PbTe/Sb_2Te_3$ lamellae. This is mainly due to the increase in carrier concentration. It is also found that the electrical resistivity is not significantly affected in the coarsening process.

Thermal conductivity

Figure 4 shows the temperature dependence of thermal conductivity of sample B, which was annealed at 773 K for 1 h, 24 h and 126 h. The thermal conductivitivities (κ_{tot}) were calculated from the measured thermal diffusivity (α), the measured density (ρ), and the heat capacity (C_P) evaluated by Dulong-Petit law using the relation, $\kappa_{tot} = \rho C_P \alpha$. The electron part of the thermal conductivity, κ_{el} was evaluated by the Wiedemann-Franz law, $\kappa_{el} = LT/\rho$, where L is Lorenz number,

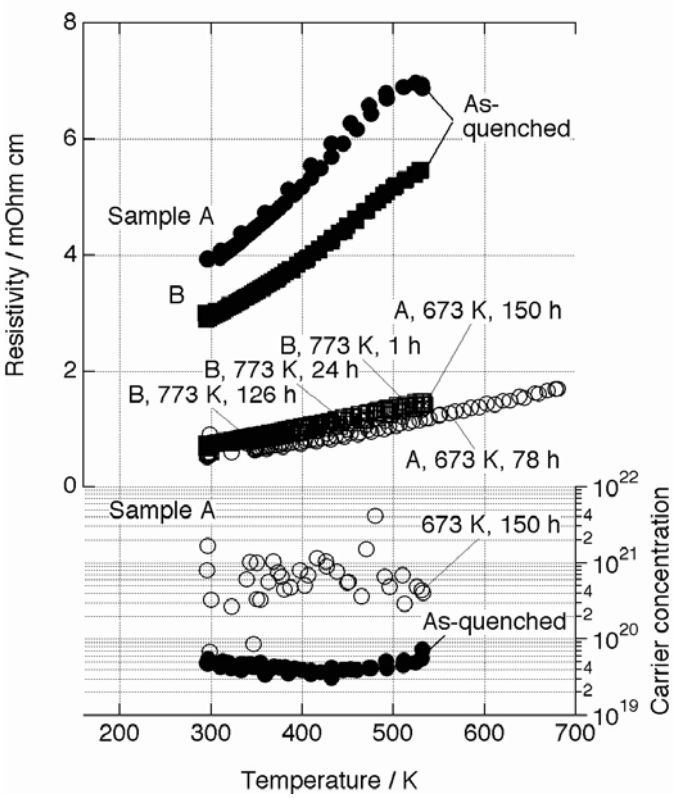

Figure 3: Electrical resistivity and carrier concentration of $Pb_{10.5}Sb_{31.6}Te_{57.9}$ in the as-quenched state and after annealings at 673 K or 773 K.

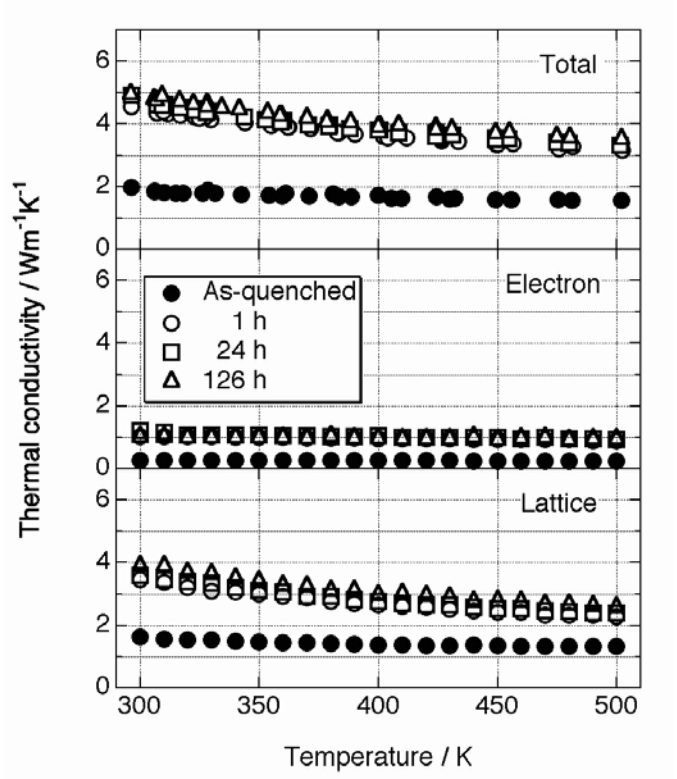

Figure 4: Total, electronic part, and lattice part of the thermal conductivity of $Pb_{10.5}Sb_{31.6}Te_{57.9}$ in the as-quenched state and after annealing at 773 K.

2.45×10^{-8} Ω/K^2. The lattice part of the thermal conductivity, κ_{lat}, was calculated using $\kappa_{tot} = \kappa_{el} + \kappa_{lat}$. The lattice part of the thermal conductivity in the as-quenched state, *i.e.* that of $Pb_2Sb_6Te_{11}$, is significantly lower than those after the decomposition. While the electrical resistivity is almost constant after annealing for 1 h at 773 K, the thermal conductivity slightly increases. As seen in the figure, this is due to the increase of lattice component of the thermal conductivity. Table 1 shows that the microstructure is coarsened by annealing. This is qualitatively consistent with the previous work [8]. Thus, the increase in the lattice part of the thermal conductivity could be attributed to the lowering of phonon scattering at phase boundaries since the coarsening of microstructure is accompanied by the decrease in the total area of phase boundaries. Actually, as seen in Fig. 5, for samples annealed at 673 and 773 K, the lattice thermal conductivity decreases with decreasing inter-lamellar spacing. Measurements are underway to add more data points to this plot, e.g., data from samples annealed at 573K.

It has previously been reported that adjacent Sb_2Te_3 and PbTe lamellae are oriented such that the close-packed planes, the <001> basal planes of Sb_2Te_3, and the <111> planes of PbTe are parallel and the lattice mismatch is only about 6% [7]. Therefore, the mass contrast due to the difference of phases or strain in the vicinity of phase boundaries could be the cause of the scattering of the phonon components which have the mean free path in similar orders of magnitude to the inter-lamellar spacing. On the other hand, electrical conductivity was not affected by the inter-lamellar spacing. This is possibly because the lattice mismatch at the interface is fairly small.

It is interesting to note that the lattice thermal conductivity of $Pb_2Sb_6Te_{11}$ is low (1.15 – 1.69 W/mK). The period of similar atomic stacking within a unit cell of $Pb_2Sb_6Te_{11}$ was taken to be 1.4 nm [9]. The $Pb_2Sb_6Te_{11}$ phase is highly disordered in the cationic substructure; however, the Sb_2Te_3 and PbTe phases are significantly more ordered. The low thermal conductivity of $Pb_2Sb_6Te_{11}$ may be due to one two possibilities: (a) disorder in the metallic sites [9] and (b) the small layer period and consequent increase in the total area of the "interfaces" of the crystalline layers.

Conclusions

$Pb_{10.5}Sb_{31.6}Te_{57.9}$ (the composition corresponding to $Pb_2Sb_6Te_{11}$) samples were prepared by solidification processing using a copper mold. After the solidification, the samples were mainly composed of $Pb_2Sb_6Te_{11}$. $Pb_2Sb_6Te_{11}$ was decomposed to PbTe and Sb_2Te_3 by annealing at 673 or 773 K. The fraction transformed and the inter-lamellar spacing (540-1600 nm) were controlled by annealing period. The electrical resistivity and the thermal conductivity were measured before and after annealing. The inter-lamellar spacing in the samples used in the property measurements was in the range between 540 and 1590 nm. It was found that the electrical resistivity is the highest for $Pb_2Sb_6Te_{11}$ (without annealing).

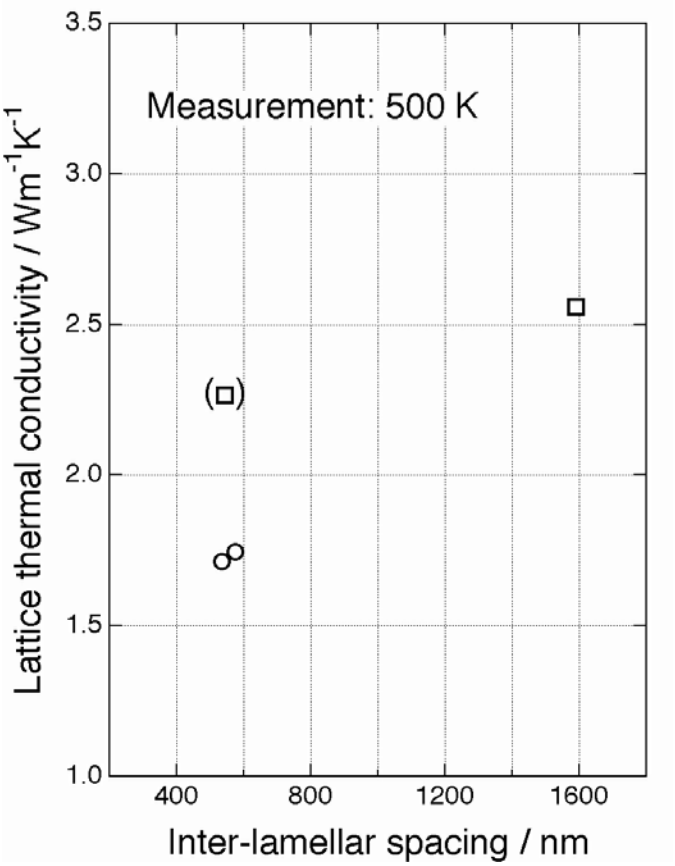

Figure 5: The dependence of lattice thermal conductivity of $PbTe/Sb_2Te_3$ lamellar composites and $Pb_2Sb_6Te_{11}$ at 500 K on inter-lamellar spacing. Circles and Squares show the results from samples sample A and B, respectively. The point of sample B for smaller inter-lamellar spacing is in brackets since the decomposition is not complete (Y = 88.7 %).

Then, the electrical resistivity decreases as the decomposition to $PbTe/Sb_2Te_3$ lamellae proceeds. The thermal conductivity increases as the decomposition proceeds and the resulting nanostructure is coarsened. The lattice thermal conductivity decreases with decreasing the inter-lamellar spacing. Further reduction in lattice thermal conductivity should be observed for even finer microstructure which we can achieve with lower temperature anneals. The self-assembled nanostructure is achieved even in bulk materials. This would greatly reduce interface problems of sublattice materials such as a relatively large electrical resistance and also simplify production processes.

Acknowledgments

This work was supported by the Office of Naval Research and Jet Propulsion Laboratory.

References

1 Caylor, J. C. *et al.*, "Enhanced Thermoelectric Performance in PbTe-based Superlattice Structures from Reduction of Lattice Thermal Conductivity," *Appl. Phys. Lett*. Vol. 87 (2005), p. 023105.

2 Venkatasubramanian, R. et al., "Thin Film Thermoelectric Devices with High Room-Temperature Figures of Merit," *Nature* 413 (2001), pp. 597-602.

3 Harman, T. C. *et al.*, "Quantum Dot Superlattice Thermoelectric Materials and Devices," *Science* Vol. 297 (2003), pp. 2229-2232.

4 Chen, G., Proc Ninth Intersociety Conference on Thermal and Thermomechanical Phenomena In Electronic Systems 2004 (IEEE Cat. No.04CH37543); p.8.

5 Abrikosov, N. K. *et al*., "The System PbTe-Sb_2Te_3," *Inorg. Mater.* Vol. 1 (1965), pp. 1944-1946.

6 Ikeda, T. *et al*., "Solidification Processing of Alloys in the Pseudo-binary PbTe–Sb_2Te_3 System," *Acta Mater.* Vol. 55 (2007), pp. 1227-1239.

7 Ikeda, T. *et al*., "Self-Assembled Nanometer Lamellae of Thermoelectric PbTe and Sb_2Te_3 with Epitaxy-like Interfaces," *Chem. Mater*. Vol. 19 (2007), pp. 763-767.

8 Ikeda, T. *et al*., "Development and Evolution of Nanostructure in Bulk Thermoelectric Pb-Te-Sb Alloys," *J. Electr. Mater.*, in press.

9 Shelimova, L. E. *et al*., "Synthesis and structure of layered compounds in the PbTe-Bi_2Te_3 and PbTe-Sb_2Te_3 systems," *Inorg Mater*. Vol. 40 (2004), pp. 1264-1270.